Substitutional Nitrogen in Nanodiamond and Bucky-Diamond Particles

A. S. Barnard*,†,‡ and M. Sternberg‡

Center for Nanoscale Materials and Materials Science Division, Argonne National Laboratory, 9700 South Cass Ave, Argonne, Illinois 60439

Received: May 9, 2005; In Final Form: July 14, 2005

The inclusion of dopants (such as nitrogen) in diamond nanoparticles is expected to be important for use in future nanodevices, such as qubits for quantum computing. Although most commercial diamond nanoparticles contain a small fraction of nitrogen, it is still unclear whether it is located within the core or at the surface of the nanoparticle. Presented here are density functional tight binding simulations examining the configuration, potential energy surface, and electronic charge of substitutional nitrogen in nanodiamond and bucky-diamond particles. The results predict that nitrogen is likely to be positioned at the surface of both hydrogenated nanodiamond and (dehydrogenated) bucky-diamond, and that the coordination of the dopants within the particles is dependent upon the surface structure.

1. Introduction

Recent decades have seen great advances in the field of nanoscience and nanotechnology, but the next generation of nanomaterials must have predictable structural, electronic, and chemical properties. The well-documented thermal, mechanical, and electronic properties of the various allotropes of carbon, along with their chemical compatibility with other types of nanomaterials, make nanocrystalline diamond-based nanodevices an attractive prospect for various applications.[1] Since the successful doping of macroscopic (bulk) diamond has led to the invention of many electronic and optoelectronic devices,[2] the inclusion of stable dopants within isolated diamond nanomaterials[3,4] and nanocrystalline diamond films grown using chemical vapor deposition (CVD)[5] is a topic of research that is currently receiving considerable attention from many groups around the world.

For electronic applications the common objective in the doping of diamond is the production of p-type and n-type semiconductor materials. In bulk diamond, nitrogen is known to be a (deep) donor,[6] and is currently a preferred candidate for n-type materials. Nitrogen-doped diamond exists in nature (type I), and a study has been previously undertaken in the doping of natural diamond, by diffusion of nitrogen into natural Type IIa diamond.[7]

With the advent of nanocrystalline diamond thin films,[8−13] with grain sizes in the order of ∼5−50 nm (depending upon growth conditions), there has been growing interest in the doping of such materials for electronic purposes. Much attention has been dedicated to the inclusion of nitrogen[14,15] in nanocrystalline diamond thin films (for the purposes of making n-type, as described above). The success of such doping will be largely dependent upon the positions of the dopants within the films, and the nature of the bonding of the dopant atoms to the surrounding carbon atoms. Computational studies investigating the configuration and bonding of nitrogen within the ultrananocrystalline diamond films (UNCD) indicated that nitrogen is likely to be located in the grain boundaries (as opposed to the grains),[16] a prediction that is consistent with preliminary experimental results.[15]

The case of particulate nanodiamond produced using detonation synthesis, often referred to as detonation nanodiamond or ultradispersed diamond (UDD), is somewhat different. Detonation-induced transformations of powerful explosives and their mixtures with the composition $C_aH_bN_cO_d$ with a negative oxygen balance in a non-oxidizing medium yield a number of condensed carbon phases, including diamond nanoparticles.[17] These particles are usually around ∼2−6 nm in diameter, with either a hydrogenated surface or a fullerenic outer shell (then denoted as "bucky-diamond"). Although most commercial diamond nanoparticles contain a small fraction of nitrogen (usually between 1% and 4%[17,18] but sometimes as high as 7−8%[19]) there is still some conjecture as to the bonding of nitrogen in nanodiamond and bucky-diamond. This includes the fundamental question of whether it will be located within the core or at the surface of nanoparticles.[17]

There are a number of experimental works that report nitrogen positioned preferentially at the surface of UDD;[17] however, it should be pointed out that gaseous N_2 or nitric acid are often used during purification.[18,19] Both as-grown and annealed samples of UDD have exhibited XPS spectra with peaks consistent with both N-sp^3 and N-sp^2 bonds, but a comparison of the N/O ratio in the samples indicated that nitrogen−oxygen groups desorbed during annealing. This again supports the hypothesis that N atoms are localized near the surface. However, other studies have found evidence of nitrogen being imbedded within the core of nanodiamonds.[20,21] These results are supported by two-phonon-excited luminescence specta (showing peaks indicative of N2 and N3 defects)[20] and electron field emission studies,[21] respectively. In general, these seemingly contradictory results make the theoretical study of the configuration of nitrogen in nanodiamond of great interest.

The study of such dopants in particulate nanodiamond is also considered important since encapsulated atoms in endofullerenes and doped nanodiamonds have been suggested as candidates of use as qubits for quantum computing.[22] The main objective in this case is to find "stable" dopants with suitable

* Address correspondence to this author. E-mail: amanda.barnard@anl.gov. Fax: +1 630 252 9555.
† Center for Nanoscale Materials.
‡ Materials Science Division.

10.1021/jp0524126 CCC: $30.25
Published on Web 08/19/2005

spin states;[22] but before the electronic or spin properties of impurities in nanodiamond may be examined, it is first important to establish which dopant species may be expected to be stable at given sites within the nanodiamond lattice. For a dopant in nanodiamond to be considered stable in this context[22] it must be included substitutionally, and it must exhibit negligible diffusion to the nanocrystallite surface.

In this paper density functional tight binding calculations are used to model the configuration, energetics, and charge distribution of substitutional nitrogen in nanodiamond and bucky-diamond particles. The results predict that it is energetically preferable for nitrogen to be positioned at the surface of both hydrogenated nanodiamond and (dehydrogenated) bucky-diamond, and that the coordination of the dopants within the particles is dependent upon the surface structure.

2. Computational Methods

The density functional based tight binding method with self-consistent charges (SCC-DFTB)[23,24] is a two-center approach to density functional theory (DFT). Formally, the Kohn−Sham density functional is expanded to second order around a reference electron density. The reference density is obtained from self-consistent density functional calculations of weakly confined neutral atoms within the generalized gradient approximation (GGA). The confinement potential is optimized to anticipate the charge density and effective potential in molecules and solids. A minimal valence basis is established and one- and two-center tight-binding matrix elements are calculated (rather than fitted) within DFT. A universal short-range repulsive potential accounts for double counting terms in the Coulomb and exchange-correlation contributions as well as the internuclear repulsion. Self-consistency is included at the level of Mulliken charges.

This method has been selected for use here as it has previously been shown to provide good agreement with higher level quantum chemical methods for carbon−nitrogen systems (such as the interaction of CN with diamond surfaces[25]), and it facilitates the examination of larger structures that are currently inaccessible using first principles methods.

3. Discussion of Results

We used this technique to model the substitutional nitrogen in isolated nanodiamond and bucky-diamond particles, consisting of 837 carbon atoms each, with a truncated-octahedral morphology (as illustrated in Figure 1a). This morphology has been identified as a low-energy shape[26] that offers a combination of {100} and {111} surfaces, {100}/{111} and {111}/{111} edges, and {111}/{111}/{100} corners. The nanoparticles measure ∼2.2 nm in diameter, a size (within the nanodiamond "window" of stability[27]) that occupies the boundary of stability for bucky-diamond and dehydrogenated nanodiamond.[28] Both dehydrogenated (C_{837}) and fully hydrogenated ($C_{837}H_{252}$) structures were constructed, and fully relaxed using the conjugate gradient scheme to minimize the total energy. The convergence criterion for a stationary point is 10^{-4} au ≈ 5 meV/Å for forces.

The $C_{837}H_{252}$ nanoparticle remained in the diamond structure upon relaxation, with the {100} surfaces relaxing to form the (2 × 1) reconstruction, as shown in Figure 1b. The C_{837} nanoparticle exhibited delamination of the {111} surfaces and {111}/{111} edges upon relaxation, thereby becoming a bucky-diamond as shown in Figure 1c. The outer surface/shell remained anchored to the core along {111}/{100} edges, and the {100} surfaces reconstructed to form the (2 × 1) surface structure, in full agreement with results of previous studies obtained using first principles methods.[29,30] Both particles underwent minor full-particle contractions, resulting in average C−C bonds in the core region of approximately 1.53 Å.

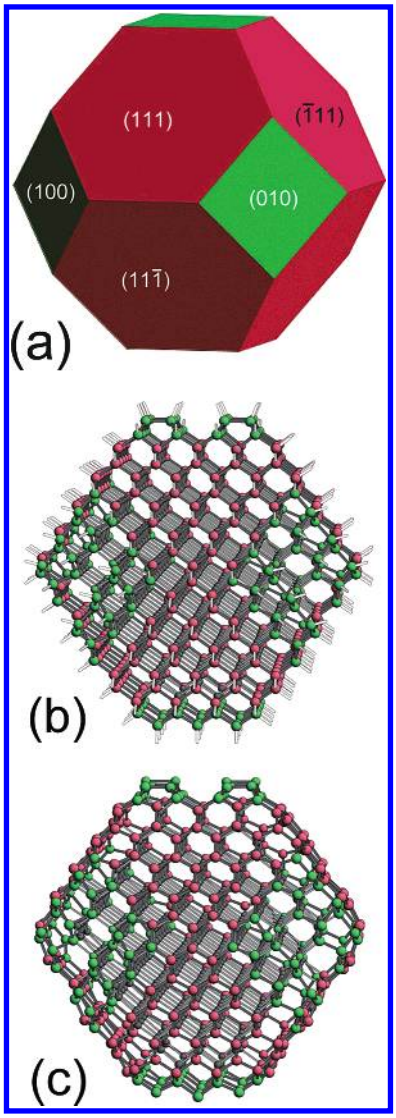

Figure 1. A schematic representation (a) of the truncated octahedral morphology considered herein, along with structural diagrams of the fully relaxed (b) hydrogenated nanodiamond particle with reconstructed (100)−(2 × 1) faces, and (c) bucky-diamond with delaminated (111) faces. The atoms participating in {111} surfaces are shown in red, and atoms participating in the {100} surfaces are shown in green (with hydrogen terminations of the nanodiamond are indicated as "sticks").

The fully relaxed C_{837} and $C_{837}H_{252}$ nanoparticles were then used as initial configurations for the subsequent calculations involving the inclusion of nitrogen dopants. In both cases, single nitrogen atoms were substituted for carbon atoms located along specific (albeit zigzagged) substitution paths within the lattice, extending from the centrosymmetric atom to different points on the surface. The directions of these substitution paths are shown in Figure 2a: denoted as A, B, C, D, and E, for substitution paths terminating at the center of the {100} surface, {111} surface, {100}/{111} edge, {111}/{111} edge, and the {111}/{111}/{100} corner (respectively). Sample substitution paths (A, C, and D) are shown in Figure 2b. If we consider the nanoparticle morphology as analogous to the shape of the diamond Brillouin zone, the substitution paths (A, B, C, D, and E) begin at the Γ point and extend along the X, L, U, K, and W directions, respectively.

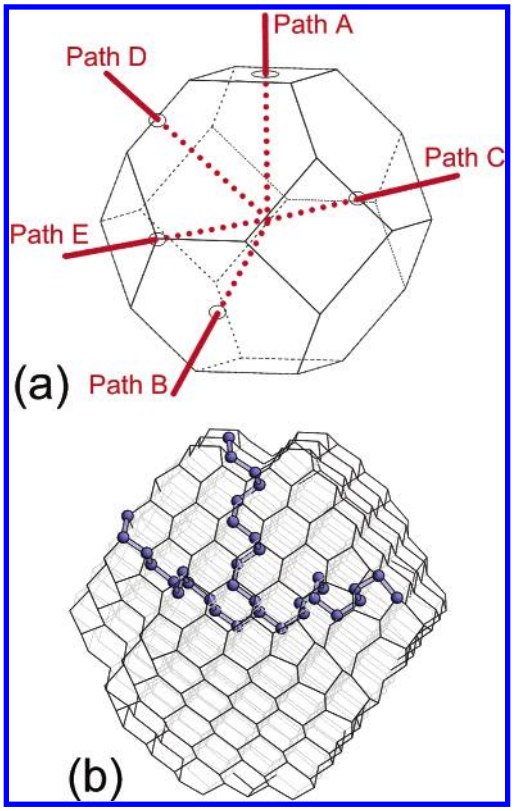

Figure 2. A schematic representation of the substitution paths examined in the bucky-diamond and nanodiamond particles (a), along with sample substitution paths shown explicitly for the cases of A, C, and D (b).

At each lattice site along these substitution paths, the nitrogen dopant and the first and second nearest neighboring carbon atoms were re-relaxed, again to a force convergence of 10^{-4} au. Initial tests, along with the results of previous studies using first principle methods[6] have shown that the disruptive influence of nitrogen within the diamond lattice is localized, and consideration of first and second nearest neighbors is sufficient to model this defect.

These tests were performed on the $C_{837}H_{252}$ nanoparticle with the nitrogen dopant at the centrosymmetric lattice site. An increasing number of atoms from successive neighbor "shells" surrounding the dopant were included in a relaxation procedure, starting out from the fully relaxed geometry of the particle before doping. The resulting energy of the re-relaxed doped particle as a function of the number of movable atoms n is shown in Figure 3, normalized to the energy for the unconstrained case $n = 1089$. We can see that including only out to the second nearest neighbor shell affects the total relaxation energy by merely 0.19 eV. This is considerably less than the defect energy due to inclusion of the nitrogen atom of 8.96 eV. Moreover, this deviation is expected to be of the same order and magnitude for all substitutional sites.

In the following sections, structure and energetics of the nitrogen along each of these substitution paths are compared and the energetically preferred location and configuration of nitrogen in nanodiamond and bucky-diamond particles identified. This is followed by an analysis of the charge distribution surrounding these sites in both particles.

3.1. Nanodiamond. In the case of the relaxed hydrogenated nanodiamond, the nitrogen dopant was found to prefer a 3-fold coordinated configuration, irrespective of location. When located at the extremum of each substitution path, this corresponds to two C−N bonds and one N−H bond. This is not surprising,

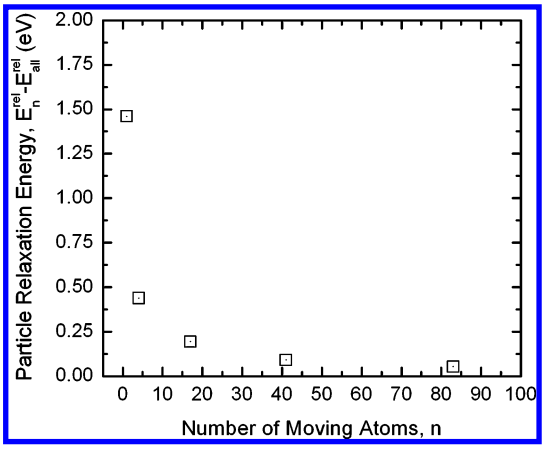

Figure 3. The total energy of the re-relaxed doped particle as a function of the number of movable atoms (n) normalized to the energy for the unconstrained case of $n = 1089$. The energetic consequence of the second nearest neighbor shell approximation to the total energy of the 2.2 nm nanoparticle is shown to be only 0.19 eV.

since nonplanar 3-fold-coordinated N has been found to be favored for substitutional N in bulk diamond.[31] Energetically, the results show a more interesting relation between the energy $E - E_{center}$ (given as the total energy of the nanoparticle relative to the energy of the nanoparticle with the dopant in the centrosymmetric position) and the substitutional site of the dopant. This is best described in Figure 4a, where the x-axis represents a scaled (dimensionless) nanoparticle radius obtained by dividing the distance from the center to the dopant site (r_X) by the total distance from the center to the extremum (R_X) in the corresponding direction (X). Hence $r/R = 0$ is the center, and $r/R = 1$ is the outermost dopant site located on an extremum (surface, edge, or corner), and bound to a hydrogen termination.

It is clear from Figure 4a that there is little energetic difference between the substitution paths in the core region of the particle, i.e., between 0 and ∼50% of the distance from the center. In this region the dopant sites are energetically indistinguishable, a fact that can be used to characterize the extent of the core region and give some indication of the fraction of the particle that may be reasonably considered as "bulk-like". Beyond this distance the general trend is toward lower energies, indicating that (in general) it is energetically preferable for nitrogen to be located near the surface of the nanodiamond.

More specifically, the results show that substitution paths D and E exhibit a smooth decrease in energy (which is proportional to $(r/R)^3$) as the sites approach the {111}/{111} edge and the {111}/{111}/{100} corner. The extremities of these substitution paths are ∼1.5 eV lower in energy than the centrosymmetric site. In contrast, substitution paths A, B, and C exhibit only a smaller decrease in energy (of ∼0.5 eV) between the center and the "subsurface" sites, followed by a further ∼1−2 eV reduction until nitrogen is located at the extremum (and bound to a hydrogen atom). The extremum of substitution paths A and C are the lowest energy sites, where (in both cases) the nitrogen atom participates in a (100)−(2 × 1):H surface dimer.

As a further check of the "second nearest neighbor shell" approximation outlined above, the extremum of substitution path C was also re-relaxed with all atoms allowed to move. The resulting difference in total energy for the nanoparticle was found to be 0.09 eV. This is even less than the value for the centrosymmetric dopant site (0.19 eV), since the nitrogen atom and its neighbors have more freedom to relax into the vacuum and have less propensity to disrupt the carbon atoms in the third or fourth neighbor shells. Therefore the second nearest neighbor

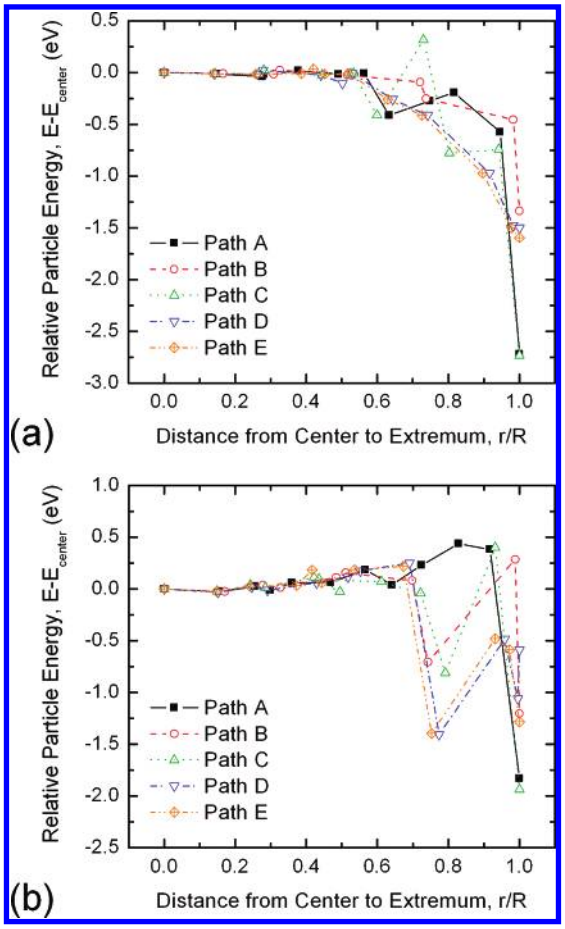

Figure 4. The relative nanoparticle energy $E - E_{center}$ for each substitutional site of the N dopant in (a) the hydrogenated nanodiamond and (b) the bucky-diamond. The dimensionless nanoparticle radius r/R is obtained by dividing the distance from the center to the dopant site by the total distance from the center to the extremum (for each direction). Hence $r/R = 0$ is the center, and $r/R = 1$ is the outermost dopant site located on an extremum (for each substitution path).

shell approximation is in fact more reliable at the surface of the nanoparticle than in the core.

3.2. Bucky-Diamond. In the case of bucky-diamond, with the exception of the central region of the core, the results show a gradual increase in energy for nitrogen substitution sites approaching the "inner-surface" of the bucky-diamond core, as shown in Figure 4b. This is followed by a sharp decrease in energy for dopant sites located on the "inner-surface" (approximately 75% of the distance from the center).[32] The increase in energy in the core region continues for sites located along substitution path A, since there is no surface delamination (and therefore no inner-surface) in this direction. The extremum of substitution paths A and C are again the lowest energy sites, due to their participation in (100)−(2 × 1) surface dimers.

The two outermost data points for paths B−E are representative of nitrogen atoms situated in the fullerenic shell of the bucky-diamond, formed by delamination of two surface atomic layers.[33] The two sites within that shell (for each substitution path) are located at approximately the same radial distance but are structurally and energetically inequivalent. In the range $r/R = \sim 0.75-1.00$ in Figure 4b the points with lower energy correspond to lattice sites in the shell that before delamination formed the outermost atomic layer (exposed to vacuum and with a "dangling bond" oriented outward). The points with higher energy correspond to sites that formed the second outermost atomic layer and had a covalent bond oriented inward, which is broken during the delamination.

TABLE 1: Net Mulliken Charges for the Extremum and Central Substitutional Sites in the Undoped and Doped Bucky-Diamond (Dehydrogenated) Nanoparticles[a]

	net charge		
site	C	N	(N−C)
A	−0.96	−0.71	+0.26
B	+0.22	−0.41	−0.64
C	−0.99	−0.76	+0.22
D	−0.34	−0.20	+0.14
E	−0.52	−0.31	+0.20
center	+0.01	+0.31	+0.30

[a] The last column gives the difference.

The *coordination* of N dopants in the bucky-diamond was found to be insensitive to the substitution path, but rather to depend on the distance from the center. Within the core the dopants were found to be 4-fold coordinated, and 3-fold coordinated in the shell. This correlates with the general "flattening" of the atomic layers on the inner surface of the bucky-diamond core and all subsequent outer layers comprising the shell. This type of flattening is consistent with previous studies of bucky-diamonds, using first principles methods.[29] Note that as a result of the flattening the substituents are distributed unevenly along the radial direction, especially between $r/R = \sim 0.75-0.9$ for paths B−E in Figure 4b, when compared to nanodiamond as shown in Figure 4a. This range corresponds to the core−shell separation distance of the bucky-diamond at ∼2.4−2.6 Å.

3.3. Distribution of Charge at Preferred Sites. Atoms in the nanoparticle, in particular those near the surface, vary greatly in their atomic environment and show a corresponding variation in their electronic configuration. Given that (for both hydrogenated nanodiamond and bucky-diamond) the energetically preferred site for nitrogen dopants is a part of a (2 × 1) dimer located either on a {100} surface (substitution path A) or a {100}/{111} edge (substitution path C), it is now prudent to examine the distribution of the excess charge associated with nitrogen atoms located at these positions. Table 1 lists the net atomic Mulliken charges of the substitution site before and after nitrogen substitution, and also their difference, defined as $\Delta c = c_N - c_{diam}$. Figure 5 illustrates these results for the N dopant and surrounding atoms (for significant cases where $|\Delta c| > 0.04$).

With the exception of the extremum of path B, the carbon atoms in the outermost substitutional sites are originally in a 3-fold nonplanar configuration with a dangling bond pointing outward. When nitrogen is substituted in these sites, the dangling bond is maintained, but the net charge is slightly less negative than in the corresponding carbon atom. Further, the first nearest neighbors of the substitutional sites are also slightly more positively charged, by about 0.1−0.2 e, and the balance is distributed across the rest of the nanoparticle. In the exceptional case of the extremum of path B, the carbon atom is part of a fullerenic segment (of a delaminated (111) surface), and thus in a 3-fold planar configuration with a slightly positive charge without a dangling bond. The nitrogen substitution leads to a puckering of the site and formation of a dangling bond, which is similar to one on the other extremum sites, as evidenced in Table 1. The surrounding carbon atoms revert from an sp^2 to an sp^3 configuration and re-bond with the diamond core. In general a weak correlation may be identified, with the lowest energy configurations also resulting in the lowest charge on the nitrogen dopant.

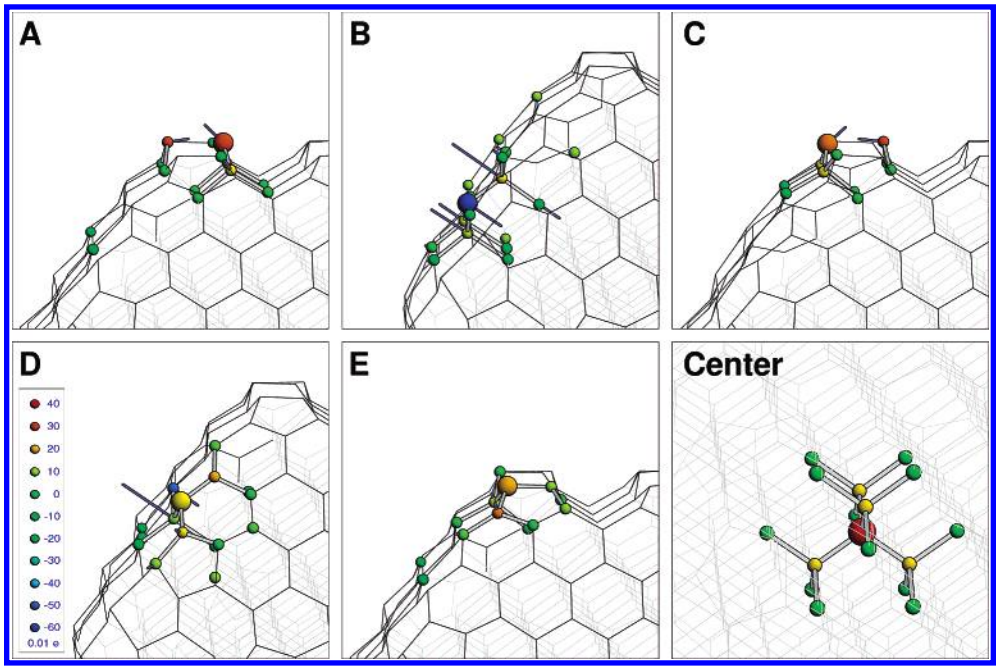

Figure 5. Atomic structure of bucky-diamond with nitrogen substitutions at the extremum for each substitution path (indicated in the top left corner of each image) and at the centrosymmetric site. The nitrogen atoms are indicated by a larger sphere. Also shown are significant changes in atomic Mulliken charges ($\Delta c = c_N - c_{diam}$), indicated by a color scale when $|\Delta c| > 0.04$. Also shown are changes in position of these atoms resulting from the re-relaxation of the dopant and surrounding neighbors ($\Delta \mathbf{R} = \mathbf{R}_{diam} - \mathbf{R}_N$), shown as 10-fold scaled vectors in blue.

4. Conclusion

Previously, a study of N in the grain boundary of UNCD was undertaken by Zapol et al.[16] using DFTB molecular dynamics, examining the electronic configuration of N dopants in a model Σ13 twist (100) grain boundary. In this study, C atoms at various sites in the interface layer of a preannealed grain boundary were substituted by N, and the annealing procedure repeated to find the optimized (low energy) configuration of the N atom. The choice of the substitutional site in a disordered structure (such as a grain boundary) is not unique, since local disorder creates a number of chemically diverse carbon atom arrangements. Four different initial single substitution N-dopant sites in the grain boundary were considered, and geometry and energetics of the final (reannealed) structures were characterized. The study determined that, in each of the four cases, the N atom relaxed to nonplanar 3-fold or 2-fold coordinated sites in the grain boundary. By calculating the formation energies for each of the N substitutions, it was shown that all four sites were energetically preferred over substitutional sites within the grains. The grain boundary dopant sites were found to be as much as 5.5 eV less than at a substitutional position within a bulk diamond lattice.

Further, to investigate the influence of nitrogen during growth of nanocrystalline diamond thin films, the energetics of CN addition to clean (reconstructed) diamond (100) surfaces was recently investigated by Sternberg et al.[25] This study used cluster models and compared results obtained by using first principles and semiempirical methods, concluding that the adsorption of CN on a diamond surface (100) is exothermic by 4.7 eV, when the CN forms a bond to a single surface atom, with the N atom oriented away from the surface.[25]

Therefore, the prediction made by the results presented herein, that substitutional nitrogen is likely to be positioned at the surface of both hydrogenated nanodiamond and (dehydrogenated) bucky-diamond as part of a (2 × 1) dimer located on a {100} surface, is considered reasonable in light of results reported by others.[16,25] Although hydrogenated nanodiamond surfaces and reconstructed bucky-diamond surface exhibit a reasonably high degree of order, whereas grain boundaries in thin films exhibit a higher degree of disorder, a unifying conclusion may be drawn by considering the crystallographic orientation of these different interfaces. Irrespective of surface structure, the degree of passivation, and the availability of undercoordinated sites, nitrogen dopants are more likely to decorate a surface than any other substitutional position in nanocrystalline diamond, a conclusion that, it is believed, may assist in guiding future theoretical and experiential studies of dopants in diamond at the nanoscale.

Acknowledgment. This work has been partially supported by the U.S. Department of Energy, Basic Energy Sciences, under contract W-31-109-ENG-38. We would also like to thank Larry Curtiss for useful discussions.

References and Notes

(1) Shenderova, O. A.; Zhirnov, V. V.; Brenner, D. W. *Crit. Rev. Solid State Mater. Sci.* **2002**, *27*, 227.

(2) Kalish, R. *Carbon* **1999**, *37*, 781.

(3) Albu, T. V.; Anderson, A. B.; Angus, J. C. *J. Electrochem. Soc.* **2002**, *149*, E143.

(4) Barnard, A. S.; Russo, S. P.; Snook, I. K. *J. Chem. Phys.* **2003**, *117*, 10725.

(5) Kaukonen, M.; Sitch, P.; Jungnickel, G.; Nieminen, R. M.; Pöykkö, S.; Porezag, D.; Frauenheim, Th. *Phys. Rev. B* **1998**, *57*, 9965.

(6) Barnard, A. S.; Russo, S. P.; Snook, I. K. *Philos. Mag. B* **2003**, *83*, 1163.

(7) Popovici, G.; Wilson, R. G.; Sung, T.; Prelas, M. A.; Khasawinah, S. *J. Appl. Phys.* **1995**, *70*, 5103.

(8) Sattel, S.; Robertson, J.; Tass, Z.; Scheib, M.; Wiescher, D.; Ehrhardt, H. *Diamond Relat. Mater.* **1997**, *6*, 255.

(9) Gruen, D. M. *Annu. Rev. Mater. Sci.* **1999**, *29*, 211.

(10) Proffitt, S. S.; Probert, S. J.; Whitfield, M. D.; Foord, J. S.; Jackman, R. B. *Diamond Relat. Mater.* **1999**, *8*, 768.

(11) Shardaa, T.; Sogab, T.; Jimbob, T.; Umenoc, M. *Diamond Relat. Mater.* **2001**, *10*, 1592.

(12) Sharda, T.; Soga, T. *J. Nanosci. Nanotechnol.* **2003**, *3*, 521.

(13) Wang, T.; Xin, H. W.; Zhang, Z. M.; Dai, Y. B.; Shen, H. S. *Diamond Relat. Mater.* **2004**, *13*, 6.

(14) Karabutov, A. V.; Konov, V. I.; Pereverzev, V. G.; Vlasov, I. I.; Zavedeev, E. V.; Pimenov, S. M.; Loubnin, E. N. *J. Vac. Sci. Technol.* **2004**, *B22*, 1319.

(15) Birrell, J.; Gerbi, J. E.; Auciello, O.; Gibson, J. M.; Gruen, D. M.; Carlisle, J. A. *J. Appl. Phys.* **2003**, *93*, 5606.

(16) Zapol, P.; Sternberg, M.; Curtiss, L. A.; Frauenheim, T.; Gruen, D. M. *Phys. Rev. B* **2001**, *65*, 045403.

(17) Dolmatov, V. Yu. *Russ. Chem. Rev.* **2001**, *70*, 607.

(18) Post, G.; Dolmatov, V. Yu.; Marchukov, V. A.; Sushchev, V. G.; Veretennikova, M. V.; Sal'ko, A. E. *Russ. J. Appl. Chem.* **2002**, *75*, 755.

(19) Aleksenskiĭ, A. E.; Osipov, V. Yu.; Vul', A. Ya.; Ber, B. Ya.; Smirnov, A. B.; Melekhin, V. G.; Adriaenssens, G. J.; Iakoubovskii, K. *Phys. Solid State* **2001**, *3*, 145.

(20) Mikov, S. N.; Igo, A. V.; Gorelik, V. S. *Phys. Solid State* **1999**, *41*, 1012.

(21) Kvit, A. V.; Zhirnov, V. V.; Tyler, T.; Hren, J. J. *Composites*: *Part B* **2004**, *35*, 163.

(22) Park, S.; Srivastava, D.; Cho, K. *J. Nanosci. Nanotechnol.* **2001**, *1*, 75.

(23) Porezag, D.; Frauenheim, Th.; Köhler, Th.; Seifert, G.; Kaschner, R. *Phys. Rev. B* **1995**, *51*, 12947.

(24) Frauenheim, Th.; Seifert, G.; Elstner, M.; Niehaus, Th.; Köhler, C.; Amkreutz, M.; Sternberg, M.; Hajnal, Z.; Di Carlo, A.; Suhai, S. *J. Phys.*: *Condens. Matter* **2002**, *14*, 3015.

(25) Sternberg, M.; Horner, D. A.; Redfern, P. C.; Zapol, P.; Curtiss, L. A. *J. Comput. Theor. Nanosci.* **2005**, *2*, 207.

(26) Barnard, A. S.; Zapol, P. *J. Chem. Phys.* **2004**, *121*, 4276.

(27) Barnard, A. S.; Russo, S. P.; Snook, I. K. *J. Chem. Phys.* **2003**, *118*, 5094.

(28) Barnard, A. S.; Russo, S. P.; Snook, I. K. *Phys. Rev. B* **2003**, *68*, 073406.

(29) Barnard, A. S.; Russo, S. P.; Snook, I. K. *Diamond Relat. Mater.* **2003**, *12*, 1867.

(30) Raty, J. Y.; Galli, G.; Bostedt, C.; Buuren, T. W.; Terminello, L. J. *Phys. Rev. Lett.* **2003**, *90*, 37402.

(31) Cox, A.; Newton, M. E.; Baker, J. M. *J. Phys.*: *Condens. Matter* **1994**, *6*, 551.

(32) Although the present study is not a diffusion or migratory study, it is clear that the inner-surface of the bucky-diamond core represents local energy minimum in the potential energy surface, which may prohibit nitrogen atoms from diffusing to the shell of the structure.

(33) Kuznetsov, V. L.; Zilberberg, I. L.; Butenko, Y. V.; Chuvilin, A. L.; Seagall, B. *J. Appl. Phys.* **1999**, *86*, 863.